Control Engineering Practice 18 (2010) 882–892

Contents lists available at ScienceDirect

Control Engineering Practice

journal homepage: www.elsevier.com/locate/conengprac

Design and implementation of parameterized adaptive cruise control: An explicit model predictive control approach

G.J.L. Naus [a,*], J. Ploeg [b], M.J.G. Van de Molengraft [a], W.P.M.H. Heemels [a,1], M. Steinbuch [a]

[a] Eindhoven University of Technology, Control Systems Technology Group, P.O. BOX 513, 5600 MB, Eindhoven, The Netherlands
[b] TNO Automotive, Advanced Driver Assistance (ADA), P.O. BOX 756, Steenovenweg 1, 5708 HN, Helmond, The Netherlands

ARTICLE INFO

Article history:
Received 19 March 2009
Accepted 24 March 2010
Available online 18 April 2010

Keywords:
Adaptive cruise control
Parameterization
Stop-&-Go
Explicit model predictive control
Quadratic programming

ABSTRACT

The combination of different characteristics and situation-dependent behavior cause the design of adaptive cruise control (ACC) systems to be time consuming. This paper presents a systematic approach for the design of a parameterized ACC, based on explicit model predictive control. A unique feature of the synthesized ACC is its parameterization in terms of key characteristics, which, after the parameterization, makes it easy and intuitive to tune, even for the driver. The effectiveness of the design approach is demonstrated using simulations for relevant traffic scenarios, including Stop-&-Go. On-the-road experiments show the proper functioning of the synthesized ACC.

1. Introduction

Adaptive cruise control (ACC) is an extension of the classic cruise control (CC), which is a widespread functionality in modern vehicles. Starting in the late 1990s with luxury passenger cars, ACC functionality is now available in a number of commercial passenger cars as well as trucks. The objective of CC is to control the longitudinal vehicle velocity by tracking a desired velocity determined by the driver. Only the throttle is used as an actuator. ACC extents CC functionality, by automatically adapting the velocity if there is a preceding vehicle, using the throttle as well as the brake system. Commonly, a radar is used to detect preceding vehicles, measuring the distance and the relative velocity between the vehicles. Hence, besides CC functionality, ACC enables also automatic following of a predecessor. In Fig. 1, a schematic representation of the working principle of ACC is shown.

ACC systems typically consist of two parts: a vehicle-independent part and a vehicle-dependent part (Moon, Moon, & Yi, 2009; Prestl, Sauer, Steinle, & Tschernoster, 2000). The vehicle-independent part determines a desired acceleration/deceleration profile for the vehicle. The vehicle-dependent part ensures tracking of this profile via actuation of the throttle and brake system. Hence, the latter part can be regarded as a controller for the longitudinal vehicle acceleration. In Fig. 2, a schematic representation of the ACC control loop is shown. The vehicle-independent part and the vehicle-dependent part form an outer and an inner control loop, respectively. This paper addresses the design of the vehicle-independent part of an ACC.

Focusing on the outer control loop, the primary control objective is to ensure following of a preceding vehicle. Considering the corresponding driving behavior, ACC systems are generally designed to have specific key characteristics, such as safety, comfort, fuel economy and traffic-flow efficiency (Vahidi & Eskandarian, 2003). In general, however, these characteristics typically impose contradictory control objectives and introduce constraints, complicating the controller design. For instance, to ensure safe following, the system should be agile, requiring high acceleration and deceleration levels, which is not desirable concerning comfort or fuel economy (Moon & Yi, 2008). To account for different characteristics, a weighted optimization can be employed. For example, a model predictive control (MPC) approach may be adopted, which also facilitates taking into account constraints (Corona & De Schutter, 2008).

Besides these key characteristics, driver acceptance of the system requires ACC behavior to mimic human driving behavior to some extent (Van Driel, Hoedemaeker, & Van Arem, 2007). Apart from the fact that human driving behavior is driver specific and time varying, it is also situation dependent. Generally, situation-dependent behavior is incorporated in the ACC in an ad-hoc manner, by switching between different modes according to different situations. This switching is either based on logic rules, using a specific tuning for each mode (Moon et al., 2009; Persson, Botling, Hesslow, & Johansson, 1999; Widmann et al.,

* Corresponding author. Tel.: +31 402474092; fax: +31 402461418.
E-mail address: g.j.l.naus@tue.nl (G.J.L. Naus).

[1] The author was partially supported by the European Community through the MOBY-DIC Project (FP7-IST-248858, www.mobydic-project.eu).

0967-0661/$ - see front matter © 2010 Elsevier Ltd. All rights reserved.
doi:10.1016/j.conengprac.2010.03.012

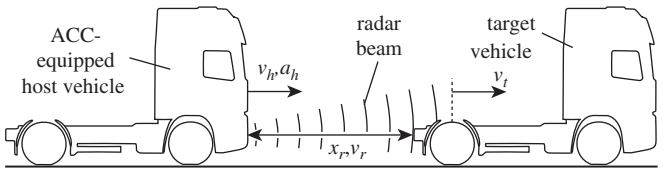

Fig. 1. Example of the ACC working principle. The host vehicle, driving with velocity v_h and acceleration a_h, is equipped with an ACC, which ensures automatic following of the preceding target vehicle, driving with velocity v_t. A radar measures the distance x_r and the relative velocity $v_r = v_t - v_h$ between the vehicles.

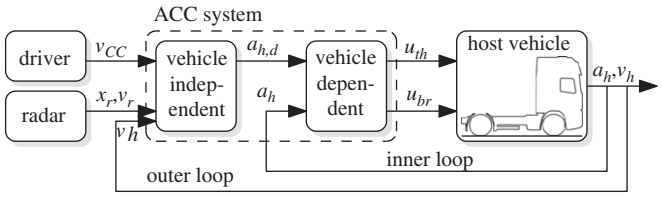

Fig. 2. Schematic representation of the ACC control loop. The ACC is divided into a vehicle-independent, outer control loop determining a desired acceleration $a_{h,d}$ and a vehicle-dependent, inner control loop determining the throttle and brake control signals u_{th} and u_{br}, respectively. The distance x_r and relative velocity v_r with respect to the preceding vehicle are measured using a radar. The driver switches the ACC on and off, regulates characteristic system settings and determines a desired cruise control velocity.

2000), or nonlinear filters are employed to combine all modes (e.g. Yanakiev, Eyre, & Kanellakopoulos, 2000; Zhang & Ioannou, 2004). Another, more crude method is to ignore specific traffic situations or consider them separately. For example, slow driving or standing still is only incorporated if so-called Stop-&-Go (SG) functionality is included (Venhovens, Naab, & Adiprasito, 2000).

The key characteristics and the desired situation dependency of the designs give rise to many tuning variables. This makes the design and tuning time consuming and error prone. In this paper, a systematic procedure for the design and tuning of the vehicle-independent part of an ACC is presented. The contribution is the design of an ACC which is parameterized by the key characteristics, with at most one tuning variable for each characteristic. Hence, after the parameterization, the specific setting of the ACC can easily be changed, possibly even by the driver. Next to presenting this systematic design approach, the implementation of the ACC and the results of on-the-road experiments are discussed.

An explicit model predictive control (MPC) synthesis is adopted to design the ACC, following Corona and De Schutter (2008) and Möbus, Baotić, and Morari (2003). One reason to use the MPC synthesis is that it enables to take into account contradictory controller requirements as well as possible constraints imposed by the key characteristics of the system. A second reason is that, when implemented in a receding horizon fashion, an optimization problem is solved in every time step. This enables the controller to adapt to actual working conditions, i.e. traffic situations, and, as such, the controller is situation dependent. For the implementation, it is desirable to solve the optimization problem offline in an explicit manner via a multi-parametric program, instead of direct online implementation of the controller. This yields an explicit, piecewise affine (PWA) control law (Bemporad, Heemels, & De Schutter, 2002; Bemporad, Morari, Dua, & Pistikopoulos, 2002).

The organization of the paper is as follows. The problem formulation is presented in Section 2. In Sections 3 and 4, the controller design and the corresponding tuning, including the parameterization of the controller are discussed. The implementation, experimental results and the working of the parameterization are presented in Section 5. Finally, conclusions and outlook on future work are given.

2. Problem formulation

2.1. Quantification measures

In this paper, safety and comfort are chosen as the key characteristics of the desired behavior of an ACC. Considering safety, however, it has to be remarked that the ACC is not a safety system such as an emergency braking system or a collision avoidance system. ACC is primarily a comfort system that incorporates safety in the sense that appropriate driving actions within surrounding traffic are guaranteed. To enable quantification of the key characteristics, desirable properties of these characteristics, so-called quantification measures, have to be defined.

The safety of the driving behavior is typically related to the inter-vehicle distance and the relative velocity of the vehicles (Naus et al., 2008). Typically, the safety of a traffic situation increases for an increasing inter-vehicle distance and a decreasing relative velocity. Furthermore, higher deceleration levels are beneficial, as a wider range of traffic situations can be handled in a safe manner. Hence, regarding safety, the inter-vehicle distance and the relative velocity will be used as quantifications measures.

The comfort of a driving action is often related to the number, size and frequency of vibrations or oscillations in the longitudinal acceleration of the vehicle due to, for example, external disturbances, engine torque peaks, driveline characteristics, etc. (Dorey, McLaggan, Harris, Clarke, & Gondre, 2001; ISO2631, 1997; Mo, Beaumont, & Powell, 1996). Besides that, specifically focusing on ACC systems, maximum deceleration values are often related to comfort (Motor Presse Stuttgart, 2006). Furthermore, the (peak) jerk levels are often considered as a measure to reflect human's comfort (Martinez & de Wit, 2007). In designing trains and elevators for example, the jerk is typically limited to $2.0\,\mathrm{m\,s^{-3}}$. Hence, regarding comfort, the (peak) acceleration and (peak) jerk levels will be used as quantification measures (Naus et al., 2008).

2.2. Parameterization

This paper presents the design of a parameterized ACC, with, at the end, only a few design parameters, i.e. tuning knobs, that are directly related to the key characteristics of the behavior of the ACC. The limited number of intuitive tuning variables enables quick and easy adaptation of the ACC to different desirable driving behavior. Importantly, these variables can also be used by non-experts in (MPC) control, like the driver, to change the behavior of the ACC system. Enabling the driver to set these variables, really makes the ACC driver dependent.

An explicit MPC approach is used to design the parameterized ACC. The MPC synthesis accommodates constraints, an optimal situation-specific controller results when implemented in a receding horizon fashing, and the minimization of a cost criterion enables making trade-offs between contradictory characteristics. However, a disadvantage of the MPC synthesis is the large number of tuning parameters, which follow from the definition of the control objective, the constraints and the choice of the cost criterion.

To obtain an ACC with only a few, intuitive design parameters, the many tuning parameters of the MPC setup are used to map the quantification measures to a few design parameters only, directly related to the key characteristics of the ACC, in this case safety and comfort. To this end, the design parameters P_s and P_c are defined, indicating to what extent the driving behavior of an ACC-controlled vehicle is either safe or comfortable, with $P_s \in [0,1]$ and $P_c \in [0,1]$, where larger values for P_s and P_c indicate an increase in safety and comfort, respectively. Incorporating P_s and P_c in the controller design yields a parameterized ACC, i.e. ACC(P_s,P_c), with P_s and P_c as tuning variables directly related to the behavior of the ACC.

Hence, depending on the driver, the design parameters P_s and P_c can be chosen to accommodate the driver's desirable setting. For comparison, in most commercially available ACC systems, the desired distance is the only parameter a driver is able to vary to adjust the behavior of the ACC. The parameterized ACC enables the driver to actually change the total behavior of the system with respect to the key characteristics. The systematic approach presented here, makes it possible to redesign the system relatively easily, for example for different key characteristics, and reduces the amount of time-consuming and error-prone trial-and-error techniques in the design. The approach is general and can be adopted for any characteristics, although focus lies on safety and comfort in this paper.

3. MPC controller design

3.1. Modeling

The MPC synthesis requires a model of the relevant dynamics to use as a prediction model. Consider the control structure as presented in Fig. 2. Focusing on the design of the vehicle-independent control part, the model should cover the longitudinal host vehicle dynamics, the vehicle-dependent control part and the longitudinal relative dynamics, which are measured by the radar. Assuming that the vehicle-dependent control part ensures perfect tracking of the desired acceleration $a_{h,d}(t)$, the internal vehicle dynamics and the vehicle-dependent control part together can be modeled by a single integrator, relating the host vehicle velocity $v_h(t)$ to the desired acceleration $a_{h,d}(t)$. This yields the following set of equations:

$$\begin{cases} x_r(t) = x_r(0) + \int_{t_0}^{t} v_r(t)\,dt \\ v_r(t) = v_r(0) + \int_{t_0}^{t} a_r(t)\,dt \\ v_h(t) = v_h(0) + \int_{t_0}^{t} a_h(t)\,dt \end{cases} \tag{1}$$

where $x_r(t)$ the relative position, $v_r(t) = v_t(t) - v_h(t)$ the relative velocity, $a_r(t) = a_t(t) - a_h(t)$ the relative acceleration, $v_h(t)$ the host vehicle velocity, and $a_h(t)$ the host vehicle acceleration at time $t \in \mathbb{R}^+$. The values of $x_r(t)$ and $v_r(t)$ are measured by the radar and measurements of $v_h(t)$ and $a_h(t)$ are available. As the acceleration of the target vehicle $a_t(t)$ is unknown, it is, for now as a nominal case, assumed to be zero for the MPC prediction model, yielding $a_r(t) = -a_h(t)$. In the end, $a_t(t)$ acts as a disturbance on the system.

The MPC algorithm is commonly designed and implemented in the discrete-time domain. Hence, the continuous-time equations (1) are converted into a discrete-time model using a zero-order hold assumption on $a_h(t)$ and an exact discretization method with sample time T_s. The signals are considered at the sampling times $t = kT_s$ where $k \in \mathbb{N}$ represents the discrete time steps:

$$\mathbf{x}(k+1) = \mathbf{A}\mathbf{x}(k) + \mathbf{B}a_h(k), \quad k \in \mathbb{N} \tag{2}$$

where $\mathbf{x}(k) = (x_r(k), v_r(k), v_h(k))^T$, and

$$\mathbf{A} = \begin{pmatrix} 1 & T_s & 0 \\ 0 & 1 & 0 \\ 0 & 0 & 1 \end{pmatrix}, \quad \mathbf{B} = \begin{pmatrix} -\frac{1}{2}T_s^2 \\ -T_s \\ T_s \end{pmatrix} \tag{3}$$

Considering the control structure as presented in Fig. 2, and assuming perfect tracking of the desired acceleration $a_{h,d}(k)$, the host vehicle acceleration $a_h(k) = a_{h,d}(k)$ can be regarded as the control input $u(k)$. Furthermore, as all states of $\mathbf{x}(k)$ are measured, the output equation becomes $\mathbf{y}(k) = \mathbf{x}(k)$, $k \in \mathbb{N}$. The total model thus becomes

$$\mathcal{M}: \begin{cases} \mathbf{x}(k+1) = \mathbf{A}\mathbf{x}(k) + \mathbf{B}u(k), \\ \mathbf{y}(k) = \mathbf{x}(k), \end{cases} \quad k \in \mathbb{N} \tag{4}$$

where $u(k) = a_h(k)$ and $\mathbf{A}$ and $\mathbf{B}$ as defined in (3).

3.2. Control objectives and constraints

Typically, the primary control objective of an ACC amounts to following a target vehicle at a desired distance $x_{r,d}(k)$. Often, a so-called desired headway time $t_{hw,d}$ is used to define this desired distance, yielding

$$x_{r,d}(k) = x_{r,0} + v_h(k)t_{hw,d} \tag{5}$$

with $x_{r,0}$ a constant representing the desired distance at standstill, and the desired headway time $t_{hw,d}$ a measure for the time it takes to reach the current position of the preceding vehicle if the host vehicle continues to drive with its current velocity, i.e. for constant $v_h(k)$. Correspondingly, the tracking error at discrete time $k \in \mathbb{N}$ is defined as $e(k) = x_{r,d}(k) - x_r(k)$. Hence, the primary control objective $\mathcal{O}_1$ comes down to minimizing the absolute tracking error $|e(k)|$, $k \in \mathbb{N}$.

Besides the primary control objective $\mathcal{O}_1$, several secondary objectives, related to the key characteristics, in this case safety and comfort, have to be included. These secondary objectives are based on the quantification measures discussed in Section 2.1. Regarding safety, the primary control objective $\mathcal{O}_1$ deals with the relative position. Besides control of the relative position, the relative velocity $|v_r(k)|$ should be made small. Regarding the comfort of a driving action, the peak values of the host vehicle acceleration $|a_h(k)|$ and jerk $|j_h(k)|$ should be kept small. Hence, next to $\mathcal{O}_1$, $|v_r(k)|$, $|a_h(k)|$ and $|j_h(k)|$ should all be small. Using the MPC setup, the objectives are incorporated in a weighted form in an optimization criterion, such that a tradeoff can be made between them.

Besides the objectives, the key characteristics introduce several constraints, which have to be included in the MPC setup. For safety, the inter-vehicle distance should always be positive, thus avoiding collisions. For comfort, the absolute value of the acceleration of the host vehicle $|a_h(k)|$ and the absolute value of the jerk $|j_h(k)|$ are constrained. The constraints on the jerk are given by $|j_h(k)| \le j_{h,max}$, where $j_{h,max}$ is an appropriately chosen positive constant. The constraints on the acceleration are more involved. For comfort reasons, high accelerations at high velocities should be prohibited. At the same time, however, quickly driving off from standstill should be possible. Hence, the constraint on the maximum acceleration $a_{h,max}$ is chosen to depend affinely on the host velocity, i.e. $a_{h,max}(v_h(k)) = a_{h,0} - \alpha v_h(k)$, where both $a_{h,0}$ and α are appropriately chosen positive constants, such that $a_{h,max}$ decreases for increasing $v_h(k)$. To guarantee safe operation with respect to erroneously detected objects, the host vehicle minimum acceleration $a_{h,min}$ is, by legislation, confined to $a_{h,min} = -3.0\,\mathrm{m\,s^{-2}}$ (ISO15622, 2002).

To accommodate the constraint on $|j_h(k)|$, as well as to enforce integral action, thus preventing steady-state errors in, for example, the following distance, the original input–output model $\mathcal{M}$ (4) is converted into an incremental input–output (IIO) model $\mathcal{M}_e$ (Maciejowski, 2002):

$$\mathcal{M}_e : \begin{cases} \mathbf{x_e}(k+1) = \mathbf{A_e}\mathbf{x_e}(k) + \mathbf{B_e}\delta u(k), \\ \mathbf{y_e}(k) = \mathbf{x_e}(k), \end{cases} \quad k \in \mathbb{N} \tag{6a}$$

where $\mathbf{x_e}(k) = (\mathbf{x}^T(k), u(k-1))^T$ the new state vector, $\delta u(k) = u(k) - u(k-1)$ the new control input, and

$$\mathbf{A_e} = \begin{pmatrix} 1 & T_s & 0 & -\frac{1}{2}T_s^2 \\ 0 & 1 & 0 & -T_s \\ 0 & 0 & 1 & T_s \\ 0 & 0 & 0 & 1 \end{pmatrix}, \quad \mathbf{B_e} = \begin{pmatrix} 0 \\ 0 \\ 0 \\ 1 \end{pmatrix} \tag{6b}$$

the new model matrices. The variation in the control output $\delta u(k)$ is now used as a measure for the jerk $j_h(k)$. Correspondingly, the constraint on the jerk is transformed into $|\delta u(k)| \le j_{h,max}$. Summarizing, the constraints are given by

$$\mathcal{C} : \begin{cases} x_{r,min} < x_r(k), \\ a_{h,min} \le u(k) \le a_{h,max}(v_h(k)), \\ |\delta u(k)| \le j_{h,max}, \end{cases} \quad k \in \mathbb{N} \tag{7}$$

where $u(k) = a_{h,d}(k) = a_h(k)$, and $x_{r,min} \le 0$ the minimal inter-vehicle distance. The model $\mathcal{M}_e$ (6) is used as the MPC prediction model in the remainder of this paper.

3.3. Control problem/cost criterion formulation

As MPC is used, a cost criterion J, which is minimized over a prediction horizon N_y, has to be defined. The future system states are predicted using the model $\mathcal{M}_e$ (6) and the current state $\mathbf{x_e}(k|k) := \mathbf{x_e}(k)$ at discrete time step k as initial condition. This yields the predicted states $\mathbf{x_e}(k+n|k)$ and the predicted tracking error $e(k+n|k)$, $n = 0,1,\ldots,N_y$ for a selected input sequence $\boldsymbol{\delta}\mathbf{U}(k|k) = (\delta u(k|k), \ldots, \delta u(k+N_y-1|k))^T$, starting at discrete time step k. Based on the prediction of the future system states, the minimization problem yields an optimal control sequence, subject to constraints (7) on the inputs and the outputs.

The cost criterion is typically formulated as a linear or as a quadratic criterion. To solve the resulting problem, the criterion is casted into a linear program (LP) or a quadratic program (QP). Finding the solution of an LP is less computationally demanding than the corresponding solution of a QP. However, the tuning of linear formulations suffers from practical drawbacks, which explains why MPC is often formulated using a quadratic criterion (Maciejowski, 2002; Rao & Rawlings, 2000). Therefore, a quadratic criterion is used, which is defined by

$$J(\boldsymbol{\delta}\mathbf{U}(k|k), \mathbf{x_e}(k)) = \sum_{n=1}^{N_y} [\xi^T(k+n|k)\mathbf{Q}\xi(k+n|k)] + \sum_{n=0}^{N_u-1} [\delta u^T(k+n) R \delta u(k+n)] \tag{8}$$

with $\xi(k+n|k) \triangleq (e(k+n|k), v_r(k+n|k), a_h(k+n|k))^T$ a column vector incorporating the control objectives, with $a_h(k+n|k) = u(k+n|k)$, and $\mathbf{Q} = \mathrm{diag}(Q_e, Q_{v_r}, Q_{a_h})$ and $R = Q_{j_h}$ the weights on the tracking error and the secondary control objectives. Furthermore, N_y and N_u denote the output and the control horizon, respectively, where $N_u \le N_y$. Moreover, for $N_u \le n < N_y$ the control signal is kept constant, i.e. $\delta u(k+n|k) = 0$ for $N_u \le n < N_y$. Finally, $u(k+n) = u(k+n-1|k) + \delta u(k+n|k)$, for $n \ge 0$.

Given a full measurement of the state $\mathbf{x_e}(k)$ of the model $\mathcal{M}_e$ (6) at the current time k, the MPC optimization problem at time k is formulated as

$$\begin{aligned} \underset{\boldsymbol{\delta}\mathbf{U}(k|k)}{\text{minimize}} \quad & J(\boldsymbol{\delta}\mathbf{U}(k|k), \mathbf{x_e}(k)) \\ \text{subject to} \quad & \text{the dynamics } \mathcal{M}_e \text{ (6)} \\ & \text{the constraints } \mathcal{C} \text{ (7)} \end{aligned} \tag{9}$$

The controller will be implemented in a receding horizon manner meaning that at every time step k, an optimal future input sequence $\boldsymbol{\delta}\mathbf{U}^*(k|k) = (\delta u^*(k|k), \ldots, \delta u^*(k+N_y-1|k))^T$ is computed in the sense of the minimization problem (9). The first component of this vector, $\delta u^*(k|k)$, is used to compute the new optimal control output $u^*(k) = u(k-1) + \delta u^*(k|k)$. This $u^*(k)$ is applied to the system, after which the optimization (9) is performed again for the updated measured state $\mathbf{x_e}(k+1) = (\mathbf{x}^T(k+1), u(k))^T$.

3.4. Explicit MPC

For the implementation, it is desirable to have an explicit MPC control law $\delta u^*(k) = \mathcal{K}(\mathbf{x_e}(k))$, instead of an implicit one obtained through online solving of the optimization problem (9) at each time step. Solving (9) as a multi-parametric quadratic program (mpQP) with parameter vector $\mathbf{x_e}$ enables an explicit form of the solution by offline optimization. The resulting explicit controller inherits all stability and performance properties of the original implicit controller and has the form of a piecewise affine (PWA) state feedback law (Bemporad, Heemels, et al., 2002; Bemporad, Morari, et al., 2002). A disadvantage of the offline optimization is that it prohibits online tuning of the controller. The controller has to be tuned offline after which a new explicit solution has to be computed, which can be implemented online.

Solving the mpQP provides a set $\mathcal{X}_f \subseteq \mathbb{R}^{n_x}$, with n_x the dimension of $\mathbf{x_e}$, of states for which the constrained optimization problem (9) is feasible. Since the control law is given by a PWA state feedback law, the feasible set $\mathcal{X}_f$ is partitioned into R polyhedral regions $\mathcal{R}_i$, $i = 1,\ldots,R$, such that

$$\mathcal{X}_f = \bigcup_{i=1}^{R} \mathcal{R}_i \tag{10}$$

where $\mathrm{int}\,\mathcal{R}_i \cap \mathrm{int}\,\mathcal{R}_j = \emptyset$, for $i = 1,\ldots,R$, $j = 1,\ldots,R$ and $i \ne j$. At time step k, the optimal input $\delta u^*(k|k)$ is then given by

$$\delta u^*(k|k) = \mathbf{F}_i \mathbf{x_e}(k) + f_i \quad \text{for } \mathbf{x_e}(k) \in \mathcal{R}_i, \ i = 1, \ldots, R \tag{11}$$

Hence, to compute the control input at discrete time step $k \in \mathbb{N}$, (11) has to be evaluated, in which the most time-consuming part is the determination of the region $\mathcal{R}_i$ that contains $\mathbf{x_e}(k)$. Implementation of the implicit controller requires solving an optimization in every time step, which is computationally often more demanding.

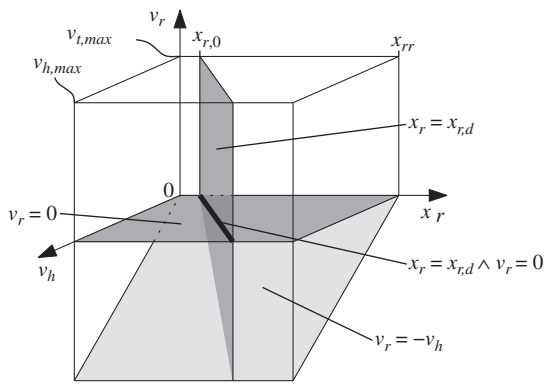

Fig. 3. Visualization of a 3D crosscut of the state space $\mathbf{x_e}$ for constant $x_{e,4} = u$, including the constraint $\mathcal{C}_i$ on the initial state (12).

The state space, which is explored when solving the mpQP, is limited by imposing a polytopic constraint $\mathcal{C}_i$ on the initial state $\mathbf{x_e}(k|k)$. This polytope is defined by

$$\mathcal{C}_i : \begin{cases} 0 < x_r(k|k) \le x_{rr} \\ 0 \le v_h(k|k) \le v_{h,max} \\ 0 \le v_t(k|k) \le v_{t,max} \\ u_{min} \le u(k-1|k) \le u_{max}(v_h(k-1|k)) \end{cases} \tag{12}$$

where x_{rr} the radar range, $v_{h,max}$ the maximum host vehicle velocity and $v_{t,max}$ the maximum target vehicle velocity. As the relative velocity is defined as $v_r(k)=v_t(k)-v_h(k)$, combination of the constraints on $v_h(k|k)$ and $v_t(k|k)$ yields a constraint on the initial state of the relative velocity $-v_h(k|k) \le v_r(k|k) \le v_{t,max}$. In Fig. 3, a crosscut at constant $x_{e,4}=u$ of the state space including the constraint $\mathcal{C}_i$ on the initial state (12) is shown.

4. Controller parameterization

4.1. Key characteristics

The MPC controller design incorporates all quantification measures regarding safety and comfort. This yields a significant number of MPC tuning parameters, given by the desired headway time $t_{hw,d}$, the constraints on the acceleration and the jerk, $a_{h,min}$, $a_{h,max}$ and $j_{h,max}$, respectively, the weights $\mathbf{Q} = \mathrm{diag}(Q_e, Q_{v_r}, Q_{a_h})$ and $R = Q_{j_h}$, and the control and prediction horizons N_u and N_y. Correspondingly, define the set Θ_{MPC}, containing the MPC tuning parameters

$$\Theta_{MPC} = \{t_{hw,d}, a_{h,min}, a_{h,max}, j_{h,max}, \mathbf{Q}, R, N_u, N_y\} \tag{13}$$

The goal of this research is to relate Θ_{MPC} explicitly to the key characteristics safety and comfort, via the design parameters P_s and P_c. These essential design parameters are directly related to the characteristics of the driving behavior, indicating to what extent the driving behavior is either safe or comfortable, with $P_s \in [0,1]$ and $P_c \in [0,1]$ (see Section 2.2).

The design of the relations between the MPC tuning parameters and the two key-characteristics related design parameters P_s and P_c is discussed in detail next. For simplicity, the control and prediction horizons are taken constant and equal, $N_y = N_u = c$. Furthermore, affine relationships are used between Θ_{MPC} on the one hand, and P_s and P_c on the other hand.

4.1.1. Operating range and benchmark measurements

Given the MPC tuning parameters Θ_{MPC} (13), the goal is to relate Θ_{MPC} explicitly to the key characteristics safety and comfort, via the design parameters P_s and P_c, yielding $\Theta_{MPC}(P_s, P_c)$. The design of these relations is based on the operating ranges of the quantification measures. These measures enable quantification of the desired properties of the key characteristics (see Section 2.2). A combination of the operating ranges of the quantification measures can be regarded as a representation of the operating range of the ACC system. Assume that the quantification measures corresponding to the key characteristics safety and comfort are contained in the sets Υ_s and Υ_c, respectively. The relations between Θ_{MPC} and the design parameters P_s and P_c are designed such that the operating ranges of Υ_s and Υ_c are mapped to the operating ranges of P_s and P_c, respectively. Remark that the operating ranges for the design parameters are defined as $P_s \in [0,1]$ and $P_c \in [0,1]$ (see Section 2.2). In this case, for simplicity, affine relationships are used between Θ_{MPC} on the one hand, and P_s and P_c on the other hand. Furthermore, the control and prediction horizons are taken constant and equal, $N_y = N_u = c$.

The design of these relations is not trivial. In general, the mapping of the operating ranges of the quantification measures Υ_s and Υ_c is not straightforwardly related to the many MPC tuning parameters, which are contained in Θ_{MPC}. For example, the setting of one tuning parameter may influence the mapping of several quantification measures. Furthermore, the mapping of a single quantification measure is, in general, influenced by the settings of several tuning parameters. Hence, the mapping of multiple quantification measures may impose contradictory requirements on the setting of a tuning parameter. In that case, a possible solution is to determine a Pareto-optimal setting for that specific tuning parameter. Instead of designing a P_s or P_c-dependent relation, this Pareto-optimal value is used as a constant setting for the tuning parameter, where it is assumed that other tuning parameters are still available to influence the mapping of the corresponding quantification measures.

The design of the relations between Θ_{MPC} and the design parameters P_s and P_c to map the operating ranges of Υ_s and Υ_c to the operating ranges of P_s and P_c, respectively, requires engineering work. Hence, the design of these relations can be regarded as a tuning step, which is done manually. However, the design has to be done only once, fixing the MPC tuning parameters Θ_{MPC} as a function of the essential design parameters P_s and P_c, being just $P_s \in [0,1]$, $P_c \in [0,1]$. As P_s and P_c are directly related to the characteristics of the driving behavior, a system with intuitive tuning knobs to change the characteristics of the ACC system with respect to the desired key characteristics, results. Other possible key characteristics such as fuel economy can be considered in an analogous manner.

The operating ranges of the quantifications measures Υ_s and Υ_c are defined by limitations and constraints following from legislation, and, in this case, safety and comfort of the driving behavior. For example, for safety, a maximum deceleration of $-3.0\,\mathrm{m\,s^{-2}}$ is defined by legislation and a minimal inter-vehicle distance $x_r > x_{r,min}$ is included in the constraints $\mathcal{C}$ (7). Considering comfortable driving behavior, the operating ranges of the corresponding quantification measures Υ_c are less clearly defined. For example, the maximum allowable acceleration or jerk for comfortable driving behavior in different situations is not specified. Consequently, these operating ranges are determined using benchmark measurements. The benchmark measurements involve on-the-road testing of various traffic scenarios by a preferably large panel of test drivers.

As benchmark measurements are used to determine the operating ranges for some of the quantification measures, the tuning depends on the test drivers. For the benchmark measurements, in this case, experiments with a commercially available ACC SG system are conducted with only a limited number of drivers. Consequently, the resulting tuning will probably not be representative for general human driver behavior, which is also not the focus of this research. Therefore, the exact tuning values will not be discussed in detail in this paper. The same holds for the tuning of the control and prediction horizons, which are, for simplicity, taken constant in this case.

4.1.2. Safety

The quantification measures related to safety are the distance and the relative velocity (see Section 2.1). The desired distance is translated into a desired headway time $t_{hw,d}$, which is typically varied between 1.0 and about 2.0 s (see e.g. Prestl et al., 2000). Human driving behavior shows a somewhat wider range, in between 0.5 and about 2.5 s (Moon & Yi, 2008). The larger the headway time, the more time the controller has to react to a certain traffic situation. Besides that, if the controller cannot handle a specific situation appropriately, the driver has more time

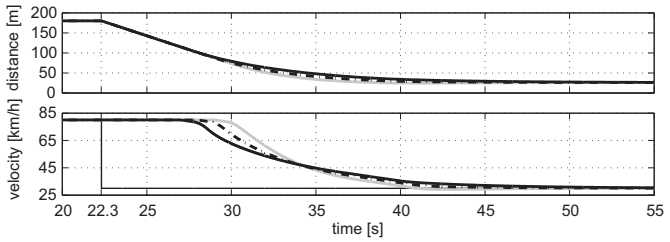

Fig. 4. The distance x_r and the host vehicle velocity v_h, corresponding to the *approach of a vehicle driving with constant velocity*. The solid black, the dash-dotted black and the solid grey lines represent the results for increasing Q_{v_r}, respectively. The narrow black line in the lower figure represents the measured target vehicle velocity v_t.

to intervene. Hence, the larger the headway time, the safer the driving will be. A corresponding relationship between $t_{hw,d}$ and P_s is $t_{hw,d}=0.5+2P_s$, yielding $t_{hw,d}\in[0.5,2.5]$, which is a sufficiently large range.

Furthermore, the weight Q_e, which is the weight on the error $e(k)$ between the desired and the actual distance, has to be considered. The larger Q_e, the smaller the time to reach a steady-state situation, i.e. $e(k)=0$, which is desirable regarding safety. A corresponding relation between Q_e and P_s is $Q_e=q_eP_s$ with $q_e\geq 0$ a positive constant. Although the focus is on safety, it has to be remarked that for increasing Q_e, the acceleration and deceleration peaks will increase as well, which indicates less comfortable driving behavior.

Finally, the relative velocity $v_r(k)$ should be minimized as fast as possible. This is influenced by the weight Q_{v_r}. For increasing Q_{v_r}, the time it takes to reach a steady-state situation in which $v_r(k)=0$ decreases, which is desirable regarding safety. However, increasing Q_{v_r} also delays the start of decreasing $v_r(k)$, which is not desirable for safety. This is shown in Fig. 4, in which the simulation results of the approach of a vehicle driving at constant velocity are shown. At 22.3 s, a preceding vehicle, which is driving slower, enters the radar range and is detected. As the results show, the time at which the controller starts decreasing $v_h(k)$ and thus $v_r(k)$ increases for increasing Q_{v_r}. Hence, whether increasing or decreasing Q_{v_r} increases or decreases the safety of the driving behavior, depends on the situation. Consequently, a constant value $Q_{v_r}=q_{v_r}$ is adopted, ensuring on average desirable behavior.

4.1.3. Comfort

The quantification measures related to comfort are the peak acceleration and jerk levels (see Section 2.1). The sizes of the weights Q_{a_h} and Q_{j_h} are naturally related to the sizes of the resulting acceleration and jerk peak values and, hence, to the amount of comfort. The higher Q_{a_h} and Q_{j_h}, the lower the corresponding acceleration and jerk peak values are and, consequently, the more comfortable the driving behavior is. This yields $Q_{a_h}=q_{a_h}P_c$ and $Q_{j_h}=q_{j_h}P_c$, with $q_{a_h}\geq 0$ and $q_{j_h}\geq 0$ positive constants. Also, the sizes of the constraint parameters $a_{h,max}(v(k))$, $a_{h,min}$ and $j_{h,max}$ are related to the amount of comfort. The smaller $a_{h,max}(v(k))$, $|a_{h,min}|$ and $j_{h,max}$, the smaller the maximum acceleration, deceleration and jerk values will be, and thus the more comfortable the driving behavior will be.

Following legislation, the maximum deceleration is limited to $a_{h,min}=-3.0\,\mathrm{m\,s^{-2}}$ (ISO15622, 2002; Van Driel et al., 2007). Analogously, the maximum acceleration is limited to $a_{h,max}=(3.0-P_c)(1-v_h(k)/v_{h,max})$, with $v_{h,max}$ the maximum vehicle velocity. This implies approximately full acceleration possibilities at low velocity, i.e. $a_{h,max}\in[2.0,\ 3.0]\,\mathrm{m\,s^{-2}}$, whereas this decreases linearly to $a_{h,max}=0.0\,\mathrm{m\,s^{-2}}$ for $v_h(k)=v_{h,max}$. As the benchmark measurements did not provide distinctive limits for $j_{h,max}$, a constant $j_{h,max}=3.0\,\mathrm{m\,s^{-3}}$ is adopted. Although the focus lies on comfort, it has to be remarked that tighter constraints on the maximum acceleration, deceleration and especially the jerk values implies that the reaction of the controller will be more sluggish, which will result in decreased safety.

4.2. Parameterization

The MPC tuning parameters Θ_{MPC} (13) are explicitly related to the key characteristics safety and comfort via the corresponding design parameters P_s and P_c, see Sections 4.1.2 and 4.1.3. As a result, the tuning of the ACC depends only on these two design parameters, as desired. Moreover, in this specific case considering comfort and safety as key characteristics, it can be assumed that the key characteristics are complementary: the design of the relations shows that for increasing safety, comfort of the driving decreases, and vice versa. For example, small acceleration and jerk peak values, indicating a high level of comfort, induce a long time to steady state, which is not desirable regarding safety. Consequently, in this case of two key characteristics, a single parameter P results:

$$P=P_c,\quad P_c+P_s=1,\quad P\in[0,1] \tag{14}$$

If more than two characteristics would be considered in the design, typically more design parameters would remain in the end.

Parameterization of the ACC with safety and comfort amounts to incorporating the relations discussed in Sections 4.1.2 and 4.1.3, accounting for (14), in the original optimization problem (9), which yields

$$\begin{aligned}&\underset{\boldsymbol{\delta}\mathbf{U}(k|k)}{\text{minimize}}\quad J(P,\boldsymbol{\delta}\mathbf{U}(k|k),\mathbf{x_e}(k))\\ &\text{subject to}\quad \text{the dynamics } \mathcal{M}_e\ (6)\quad \text{the constraints } \mathcal{C}(P)\ (7)\end{aligned} \tag{15}$$

Changing the behavior of the ACC system comes down to adjusting P. Allowing the driver to change $P\in[0,1]$ enables the driver to influence the behavior of the controller individually, focusing on either comfortable or safe driving.

4.3. Explicit solution

The total controller design is implemented via the multi-parametric toolbox (MPT) (Kvasnica, Grieder, Baotic, & Christophersen, 2006). As an explicit solution is desirable, an explicit controller is calculated offline by casting the problem as a multi-parametric program as discussed in Section 3.4. The result is a feedback control law as in (11), which is dependent on the state vector $\mathbf{x_e}(k)\in\mathbb{R}^{n_x}$ and the parameter P (14). To set the ACC to a desirable behavior according to the driver's wishes using an implicit solution, setting of P can be done online. Using an explicit solution, however, the controller has to be recomputed offline. In this case, one might store various explicit controllers for a finite number of values $P\in n/N$ for $n=0,1,2,\ldots,N$. For the multi-parametric program as discussed in Section 3.4, the number of regions in the explicit ACC laws ranges from 110 to 121. Computation of the piecewise affine maps with an Intel Pentium 2.13 GHz processor takes several seconds.

The amount of memory that is used for storing the explicit solution depends on the size of the look-up table and the number of points N that is used to discretize the continuous operating range of P. The size of the look-up table depends on the complexity of the problem, for which the number of regions in the explicit ACC laws and the dimension of the solution space, which is 4th order, are indicators. For $N=10$, a 4D solution space, and 110–121 regions per explicit ACC law, the amount of memory

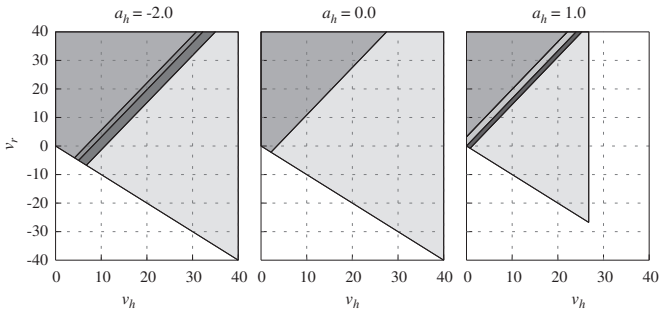

Fig. 5. Three 2D crosscuts of the solution space at constant $x_r=10\,\mathrm{m}$ for varying $x_{e,4}=a_h\in\{-2.0,0.0,1.0\}\,\mathrm{m\,s^{-2}}$.

that is required for storing the explicit solutions comes down to approximately 6500 reals. The size and complexity of the piecewise affine maps are sufficiently small for fast online evaluation.

In Fig. 5, three 2D crosscuts of the intersection $\mathcal{C}_i\cap\mathcal{X}_f$ are shown, where $x_{e,1}=x_r$ is constant, $x_{e,4}=u=a_h$ is varying, and $P=0.1$. The grey areas represent different regions $\mathcal{R}_i$ with the same affine control law. The right plot in Fig. 5 shows that the intersection $\mathcal{C}_i\cap\mathcal{X}_f$ is only a subset of $\mathcal{C}_i$, indicating that not all relevant states $\mathbf{x_e}(k)\in\mathcal{C}_i$ are feasible.

5. Implementation and results

To enable actual implementation and corresponding evaluation of the ACC, additional functionality is required, concerning CC functionality, the transition between CC functionality and ACC functionality, and warning of the driver in a potentially dangerous situation. The design of this additional functionality is discussed first, after which the setup and results of simulations and on-the-road experiments are presented.

5.1. CC functionality

The overall ACC system combines both ACC and CC functionality. For CC functionality, tracking of a desired CC velocity v_{CC} is desired. Furthermore, driving in CC mode, the ACC system should switch automatically to ACC mode in case of a preceding vehicle driving slower than this desired CC velocity.

In this paper, focus lies on the controller design for the ACC mode. To get CC functionality from this ACC design, a 'virtual target vehicle' is created, which virtually drives with a velocity equal to the desired CC velocity v_{CC} at the corresponding desired distance $x_r(k)=x_{r,d}(k,v_h(k))|_{v_h(k)=v_{CC}}$ with respect to the host vehicle. Using the virtual radar output corresponding to the position and velocity of the 'virtual target vehicle', instead of the actual radar output corresponding to a real target vehicle, the same explicit MPC solution can be used for both ACC and CC functionality. As a result, in CC mode, the same driving behavior is achieved as in ACC mode.

5.2. CC–ACC transition

For switching from ACC to CC functionality and vice versa, the common approach proposed in literature employs logic rules. Either the functionality yielding the lowest acceleration, i.e. the control input $u(k)$, is employed (Persson et al., 1999), or ACC functionality is employed if braking is required and CC otherwise (Zhang & Ioannou, 2004). To prohibit chattering, often, a boundary layer comprising hysteresis or a delay is assigned to the switching rules (Widmann et al., 2000).

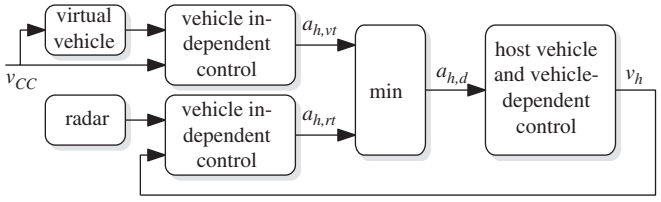

Fig. 6. Implementation of the CC–ACC transition. A virtual vehicle, driving virtually at a velocity v_{CC}, mimics radar data. The corresponding control output $a_{h,vt}$ is compared to the control output corresponding to the real radar data, $a_{h,rt}$. Based on the minimum of both control outputs, the system switches between the virtual vehicle, CC functionality, or the real radar data, ACC functionality.

The solution proposed here uses switching based on the lowest acceleration. As the acceleration is the control input, this assures smooth transitions. Both the desired acceleration following from the preceding real target vehicle, used for ACC functionality, and the desired acceleration following from the virtual target vehicle that is used for CC functionality are compared. The lowest acceleration is used as the input. This is schematically shown in Fig. 6.

5.3. Positively invariant subset

Consider the intersection of the space defined by the constraints $\mathcal{C}_i$ on the initial state and the feasible state space $\mathcal{X}_f$ (10), i.e. $\mathcal{C}_i\cap\mathcal{X}_f$. All states $\mathbf{x_e}(k)\in\mathcal{C}_i\cap\mathcal{X}_f$ are feasible, meaning that all constraints $\mathcal{C}$ (7) are fulfilled. However, only for a positively invariant subset $\mathcal{F}$ inside $\mathcal{C}_i\cap\mathcal{X}_f$, where a set $\mathcal{F}$ is called positively invariant for a system $\mathbf{x}(k+1)=\mathbf{g}(\mathbf{x}(k))$ if for all $\mathbf{x}(0)\in\mathcal{F}$ it holds that the corresponding solution to $\mathbf{x}(k+1)=\mathbf{g}(\mathbf{x}(k))$ satisfies $\mathbf{x}(k)\in\mathcal{F}$ for $k\in\mathbb{N}$, it can be guaranteed that the constraints $\mathcal{C}$ (7) are fulfilled for all times, in case the solution stays inside $\mathcal{C}_i$ and the target vehicle acceleration equals $a_t(k)=0$ for $k\in\mathbb{N}$.

This is an important aspect when implementing an ACC. For example, consider a cut-in scenario in which a vehicle, driving with a lower velocity than the host vehicle, cuts in at a small distance in front of the host vehicle. This is a feasible state. To prevent violation of the constraint on the relative position, i.e. to prevent a collision, significant braking is required. As this might be prohibited by the constraint on the maximum deceleration, one of the constraints might be violated as a result.

Consequently, take $\mathcal{F}_\infty$, the largest positively invariant subset inside the intersection $\mathcal{C}_i\cap\mathcal{X}_f$ (Kolmanovsky & Gilbert, 1997; Raković, Grieder, Kvasnica, Mayne, & Morari, 2004). For states $\mathbf{x_e}(k)\in\mathcal{F}_\infty$, it is guaranteed that all constraints will be fulfilled for all times in case the target vehicle acceleration equals $a_t(k)=0$ for $k\in\mathbb{N}$. This means that the ACC system can handle the present traffic scenario in an appropriate manner. However, for states $\mathbf{x_e}(k)\notin\mathcal{F}_\infty$, this cannot be guaranteed. At this point, the ACC system can warn the driver to take over control of the ACC system. Warning the driver in case of such a potentially dangerous situation, indicating to take over control, follows naturally from the theoretical MPC set up. The advantage of this setup is that it can be predicted if future constraint violation might occur, by detection of $\mathbf{x_e}(k)\notin\mathcal{F}_\infty$, and thus warn the driver in time.

5.4. Simulations and on-the-road experiments

A set of seven distinct scenarios, encompassing the total envelope of working conditions, is determined to evaluate the functionality of the controller, see Table 1. Based on this set of

Table 1
Envelope of traffic scenarios.

(1)	Steady following of a target vehicle with a varying velocity
(2)	Approach of a vehicle at standstill or a vehicle driving with a constant velocity, yielding a CC to ACC switch
(3)	A cut in, which involves a sudden step in x_r such that $x_r < x_{r,d}$. For $v_r < 0$ and $v_r > 0$, this is called a negative and a positive cut in, respectively
(4)	A cut out, which involves a sudden step in x_r, yielding an ACC to CC switch
(5)	Following of a decelerating vehicle to standstill
(6)	Driving away at a traffic light and following of an accelerating vehicle yielding an ACC to CC switch
(7)	Accelerating and decelerating in the CC mode due to changes in the CC velocity v_{CC}

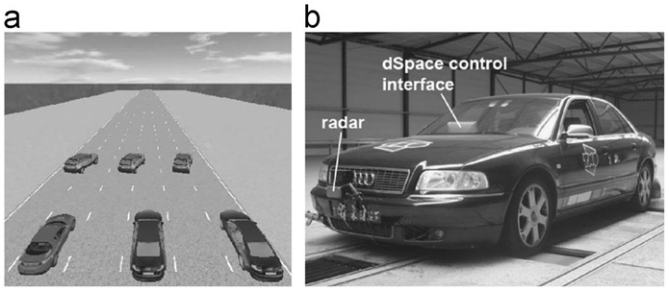

Fig. 7. (a) Screenshot of a PreScan simulation environment. Three ACC SG-equipped host vehicles and three target vehicles causing corresponding cut-in situations are shown. The ACC SG systems of the host vehicles are tuned distinctively for comparison. (b) The Audi S8 in which the ACC SG is implemented. The functionality of the controller was first tested in the TNO VEHIL test facility (TNO, 2008) before the tests in actual traffic have been performed.

scenarios, a test program is set up. Simulations are performed using the numerical tool PreScan, see Fig. 7(a) for an impression (TNO, 2008). To validate the simulation results and to enable performance evaluation, the controller has been implemented on an Audi S8 (see Figs. 7(b) and 8). If not specified otherwise, a setting $P=0.5$ is used for both the simulations and the experiments.

Implementation of the ACC system on the Audi S8 relies on the availability of the following signals. The velocity of the vehicle $v_h(t)$ is available on the CAN-bus via the built-in anti-lock braking system (ABS). The acceleration $a_h(t)$ is derived from this velocity signal. The vehicle is equipped with an electro-hydraulic braking (EHB) system, facilitating brake-by-wire control. An OMRON laser radar, i.e. a lidar, with 150 m range is built-in. Using rapid control prototyping, the ACC system is implemented on a dSpace AutoBox, with a sample rate of 100 Hz. The ACC system includes a controller for the longitudinal dynamics of the vehicle, i.e. the inner control loop in Fig. 2. A laptop is used to monitor all signals and log the data. A schematic overview of the instrumentation is shown in Fig. 8.

In Fig. 9, the results of on-the-road experiments with the Audi S8 are shown. The results correspond to driving in city traffic, showing, subsequently, steady following of a preceding target vehicle (scenario 1 of Table 1), with at about 37 s a momentarily loss of the fix of the radar on the target vehicle (the default radar output is $x_r=0$ m), which has negligible influence on the driving behavior in this case; in between 55 and 100 s, the approach of, standstill at, and, subsequently, driving off at a traffic light (scenarios 5 and 6 of Table 1); at 107 s, and several seconds later again, a cut out of the preceding vehicle, inducing a switch from ACC mode to CC mode (scenario 4 of Table 1); immediately following the cut-out situations, vehicles cut in, both times driving with a lower velocity than the host vehicle (scenario 3 of Table 1); and, finally, at 112 s, the results show again the approach of a traffic light (scenario 5 of Table 1).

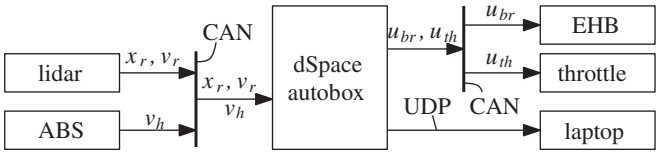

Fig. 8. Schematic overview of the instrumentation of the vehicle. The main communication channels and corresponding signals are indicated, where u_{th} and u_{br} are the throttle and brake system control signals, respectively, v_h is the host vehicle velocity, and x_r and v_r are the relative position and velocity, respectively.

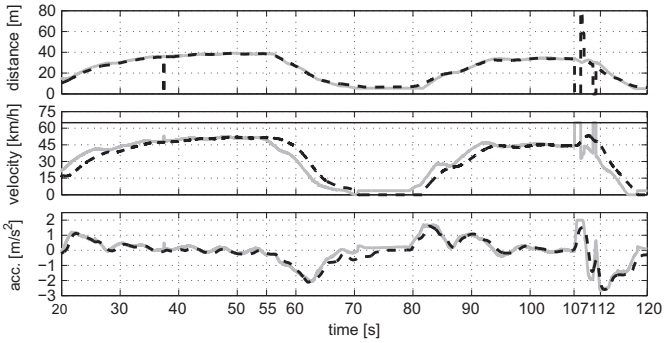

Fig. 9. Experimental results corresponding to driving in city traffic. The dashed black lines represent x_r, v_h and a_h. The solid grey lines represent $x_{r,d}$, v_t and the controller output $a_{h,d}$, and the thin solid line in the middle plot represents the desired CC velocity v_{CC}.

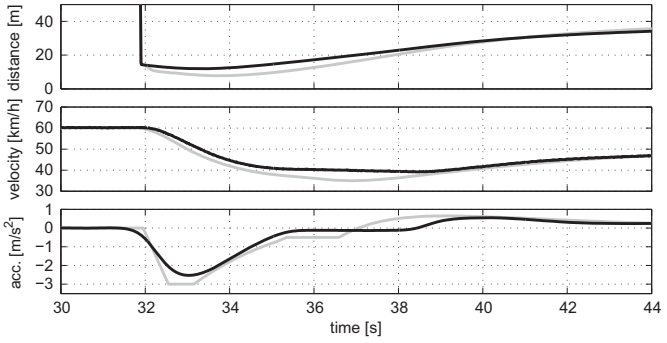

Fig. 10. The distance x_r, host vehicle velocity v_h and acceleration a_h, corresponding to a *negative cut in* (scenario 3 of Table 1). The solid black and grey lines represent the results of on-the-road experiments and simulation results, respectively.

The sensitivity of the ACC for model uncertainties and measurement noise is not specifically investigated in this research. Nevertheless, the measurement results show that the ACC is, at least to some extent, in practice, robust for model uncertainties, and that the sensitivity for measurement noise is small.

5.4.1. Simulations vs experiments

In Fig. 10, results of an on-the-road experiment and simulation results are compared. Values of the jerk $j_h(t)$ are not shown as these are difficult to obtain in practice. Regarding the simulations, for simplicity, vehicle models are not taken into account. Hence, for the simulations, $a_h(k)=a_{h,d}(k)$ holds. Although good tracking properties are normally guaranteed by the vehicle-dependent control part, exact tracking is, of course, not the case in practice. This is the main cause of the differences between the simulation and experimental results. Taking into account appropriate vehicle models in the MPC synthesis as well as the simulations would increase the resemblance between the two responses significantly.

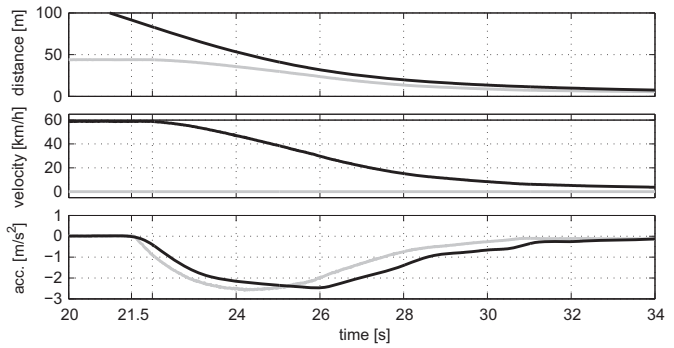

Fig. 11. Experimental results corresponding to *the approach of a standstill vehicle* (scenario 2 of Table 1). The solid black lines represent x_r, v_h and a_h. The solid grey lines represent $x_{r,d}$, v_t and the controller output $a_{h,d}$. The thin black line in the middle plot represents v_{CC}.

Nevertheless, the same characteristics can be seen in both the simulation and the experimental results. The time constants and peak values correspond fairly well. This means that the simulations can be used for the purpose of evaluation of the ACC characteristics. As the reproducibility of simulated traffic situations is better than that of real traffic situations, simulation are very useful for the comparison of the results of various settings. From this point of view, the resemblance between experimental and simulation results is satisfactory.

5.4.2. Additional functionality

The experimental results shown in Fig. 11 show the working of the CC functionality and the switching between CC and ACC functionality, see Sections 5.1 and 5.2, respectively. Experimental results corresponding to the approach of a standstill vehicle (scenario 2 of Table 1) are shown. Initially, the vehicle drives at the desired CC velocity of 60 km h^{-1}. With decreasing x_r, a desirable switch from CC to ACC functionality takes place at 21.5 s. The ACC system switches to automatic following as the target vehicle is driving at a velocity which is lower than the desired CC velocity.

5.4.3. Varying ACC behavior

To illustrate the influence of varying $P \in [0,1]$, several scenarios of Table 1 are simulated for different settings $P \in \{0.2,0.5,0.8\}$. For the sake of reproducibility, simulation results instead of experimental results are shown. The results are presented in Figs. 12–15. For increasing $P \in \{0.2,0.5,0.8\}$, the results are indicated in solid black, dash-dotted black and solid grey, respectively.

Figs. 12 and 13 show the results corresponding to following of a decelerating vehicle (scenario 5 of Table 1) and the approach of a standstill vehicle (scenario 2 of Table 1), respectively. The results in both Figs. 12 and 13 clearly indicate more comfortable behavior for increasing P. The larger P, the smaller the resulting absolute acceleration and jerk peak values are.

In case of a negative cut in (scenario 3 of Table 1), from a safety point of view, direct reaction and substantial braking are required, disregarding the setting of P. In Fig. 14, the results of a negative-cut-in scenario are shown. At 20 s, a target vehicle shows up 20 m in front of the host vehicle with a velocity of 65 km h^{-1}, while the host vehicle is driving in CC mode at 80 km h^{-1}. As a result, the host vehicle starts to brake immediately, indeed disregarding comfort-related measures such as the peak acceleration level. This indicates that safe behavior is guaranteed for any P. Furthermore, the results in Fig. 14 show that for decreasing P the desired distance increases, which is desirable regarding safety.

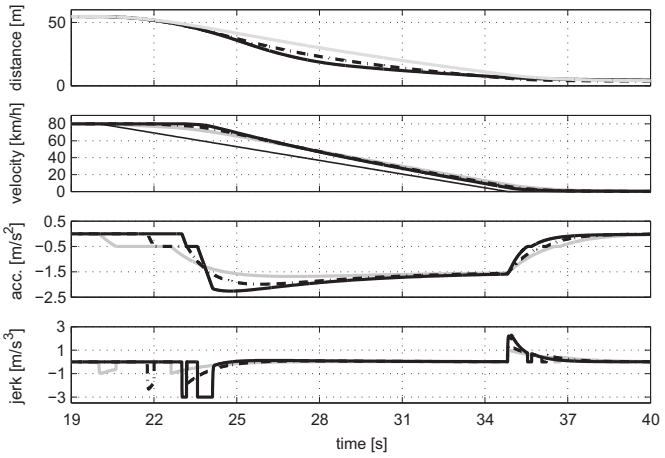

Fig. 12. Host vehicle velocity v_h, acceleration a_h and jerk j_h, corresponding to *following of a decelerating vehicle* (scenario 5 of Table 1). The solid black, dash-dotted and solid grey lines show the results for increasing $P \in \{0.2,0.5,0.8\}$.

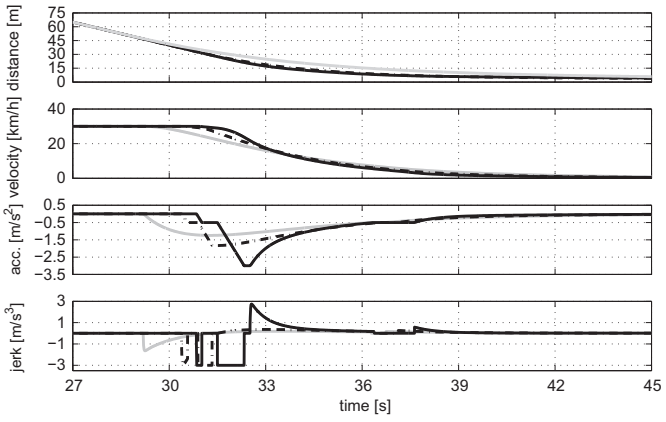

Fig. 13. Host vehicle velocity v_h, acceleration a_h and jerk j_h, corresponding to *approach of a standstill vehicle* (scenario 2 of Table 1). The solid black, dash-dotted and solid grey lines show the results for increasing $P \in \{0.2,0.5,0.8\}$.

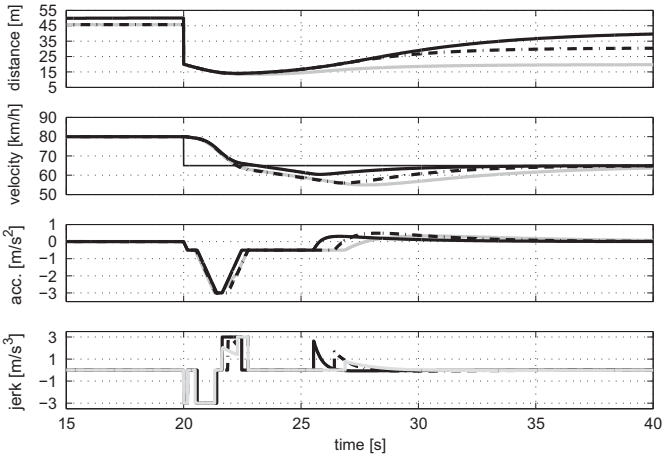

Fig. 14. The distance x_r, host vehicle velocity v_h and acceleration a_h, corresponding to a *negative cut in* (scenario 3 of Table 1). The solid black, dash-dotted black and solid grey lines represent the results for increasing $P \in \{0.2,0.5,0.8\}$, respectively. The narrow black line in the middle figure represents the target vehicle velocity v_t.

Finally, the results for a so-called cut out (scenario 4 of Table 1) are shown in Fig. 15. A preceding target vehicle changes lane, which yields an ACC to CC switch and thus acceleration to the

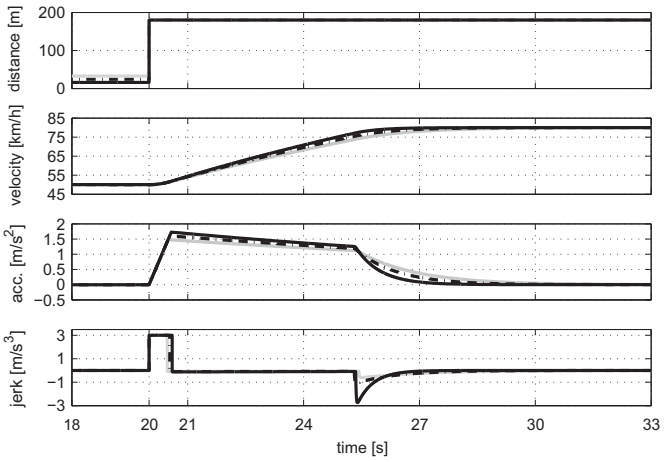

Fig. 15. Host vehicle velocity v_h and acceleration a_h, corresponding to a *cut out, yielding an ACC to CC switch* (scenario 4 of Table 1). The solid black, dash-dotted black and solid grey lines represent the results for increasing $P \in \{0.2,0.5,0.8\}$, respectively.

desired CC velocity v_{CC}. The constraint on the maximum acceleration is dependent on $P \in \{0.2,0.5,0.8\}$ as well as the host vehicle velocity $v_h(k)$, which is clearly shown.

Hence, the results presented in Figs. 12–15 show the proper working of the parameterization. By changing the setting of the design parameter $P \in [0,1]$, the behavior of the ACC system changes, with respect to the comfort and the safety of the resulting driving action. The behavior of the system is thus translated into one essential parameter P, which is directly related to the characteristics of the driving behavior.

6. Conclusions and future work

This paper presents a systematic procedure to design an ACC, which is directly parameterized by the key characteristics of the ACC behavior. The goal of the parameterization of the ACC is to reduce the time it takes to tune the system and to enable the tuning for the driver. The latter requires that the tuning should be simple and intuitive with only a few design parameters, i.e. tuning knobs, that are directly related to the key characteristics of the ACC, such as safety, comfort, fuel economy and traffic flow efficiency. In this paper, focus lies on safety and comfort, defining the design parameters P_s and P_c, respectively. To indicate the desired properties of the ACC system, quantification measures are defined corresponding to the key characteristics. The parameterized ACC is obtained by mapping the operating ranges of the quantification measures to the operating ranges of the design parameters P_s and P_c, being just $P_s \in [0,1]$ and $P_c \in [0,1]$. Due to the generality of the approach, other characteristics can be incorporated in the design, using the same systematic design procedure.

The approach is based on (explicit) MPC. MPC can handle constraints and can easily include tradeoffs between different key characteristics by appropriately selecting the cost function. In addition, MPC is suitable because its receding horizon implementation renders the ACC situation-specific, enabling mimicking of human driving behavior. This is necessary for driver acceptance of the system. The many tuning parameters of the MPC setup are used to perform the mapping of the operating ranges of the quantification measures to the design parameters P_s and P_c. This requires engineering work. However, the tuning has to be done only once, fixing the MPC tuning parameters as a function of the essential design parameters P_s and P_c, which could be united in one design parameter P in this specific case. Consequently, after this parameterization, the ACC is easy and intuitive to tune by means of a single parameter P, which is directly related to the key characteristics safety and comfort.

Simulations as well as on-the-road experiments have shown the proper functioning of the parameterized ACC for a complete envelope of working conditions: (i) the simulation results resemble the experimental results satisfactorily, (ii) additional functionality includes CC functionality, provides switching between CC and ACC functionality, and facilitates in time warning of the driver in case of a potentially dangerous situation, and (iii) changing the behavior of the system by changing the setting of the design parameter P, has proven to work in a desired manner.

Future research will focus on the design of an ACC system with different key characteristics, such as fuel economic driving or traffic flow efficiency. Furthermore, research will focus on extending the two-vehicle model to multiple vehicles. Taking vehicle-to-vehicle communication into account too, allows for the design of so-called cooperative ACC systems. The communication provides additional information concerning the surrounding traffic in addition to the radar data, which can be very beneficial to the overall system behavior.

References

Bemporad, A., Heemels, W., & De Schutter, B. (2002). On hybrid systems and closed-loop MPC systems. *IEEE Transactions on Automatic Control*, *47*(5), 863–869.

Bemporad, A., Morari, M., Dua, V., & Pistikopoulos, E. (2002). The explicit linear quadratic regulator for constrained systems. *Automatica*, *38*(1), 3–20.

Corona, D., & De Schutter, B. (2008). Adaptive cruise control for a SMART car: A comparison benchmark for MPC-PWA control methods. *IEEE Transactions on Control Systems Technology*, *16*(2), 365–372.

Dorey, R., McLaggan, J., Harris, J., Clarke, D., & Gondre, B. (2001). Transient calibration on the testbed for emissions and driveability. *SAE technical paper series* (2001-01-0215).

International Organization for Standardization (1997). *Mechanical vibration and shock—evaluation of human exposure to whole-body vibration*. NEN-ISO 2631.

International Organization for Standardization (2002). *Transport information and control systems—adaptive cruise control systems—performance requirements and test procedures*. NEN-ISO 15622.

Kolmanovsky, I., & Gilbert, E. G. (1997). Theory and computation of disturbance invariant sets for discrete-time linear systems. *Mathematical Problems in Engineering*, *4*, 317–367.

Kvasnica, M., Grieder, P., Baotic, M., & Christophersen, F. (2006). *Multi-parametric toolbox* (*MPT*).

Maciejowski, J. M. (2002). *Predictive control with constraints*. Harlow: Prentice Hall—Pearson Education Limited (ISBN: 0-201-39823-0).

Martinez, J.-J., & de Wit, C. C. (2007). A safe longitudinal control for adaptive cruise control and Stop-and-Go scenarios. *IEEE Transaction on Control System Technology*, *15*(2), 246–258.

Mo, C., Beaumont, A., & Powell, N. (1996). Active control of driveability. *SAE technical paper series* (960046).

Möbus, R., Baotić, M., & Morari, M. (2003). Multi-object adaptive cruise control. In *Lecture notes in computer science*. *Hybrid systems*: *Computation and control* (Vol. 2623, pp. 359–374).

Moon, S., Moon, I., & Yi, K. (2009). Design, tuning, and evaluation of a full-range adaptive cruise control system with collision avoidance. *Control Engineering Practice*, *27*, 442–455.

Moon, S., & Yi, K. (2008). Human driving data-based design of a vehicle adaptive cruise control algorithm. *Vehicle System Dynamics*, *46*(8), 661–690.

Motor Presse Stuttgart GmbH & Co. KG (2006). Auto Motor und Sport—Abstands-regeltempomaten: Nah dran. URL: 〈http://www.auto-motor-und-sport.de/tests/technik/hxcms_article_132252_14114.hbs〉.

Naus, G., van den Bleek, R., Ploeg, J., Scheepers, B., van de Molengraft, M., & Steinbuch, M. (2008). Explicit MPC design and performance evaluation of an ACC Stop-&-Go. In *Proceedings of the 2008 American Control Conference* (pp. 224–229), Seattle, WA, USA.

Persson, M., Botling, F., Hesslow, E., & Johansson, R. (1999). Stop & Go controller for adaptive cruise control. In *Proceedings of the IEEE international conference on control applications* (Vol. 2, pp. 1692–1697), Kohala Coast, HI, USA.

Prestl, W., Sauer, T., Steinle, J., & Tschernoster, O., 2000. The BMW active cruise control ACC. *SAE technical paper series* (2000-01-0344).

Raković, S. V., Grieder, P., Kvasnica, M., Mayne, D. Q., & Morari, M., 2004. Computation of invariant sets for piecewise affine discrete time systems

subject to bounded disturbances. In *43rd IEEE conference on decision and control* (pp. 1418–1423).

Rao, C., & Rawlings, J. (2000). Linear programming and model predictive control. *Journal of Process Control*, *10*(2), 283–289.

TNO (2008). PreScan and VEHIL (Vehicle Harware In the Loop) test facility 〈http://www.tno.nl〉. TNO Automotive, Helmond, The Netherlands.

Vahidi, A., & Eskandarian, A. (2003). Research advances in intelligent collision avoidance and adaptive cruise control. *IEEE Transactions on Intelligent Transportation Systems*, *4*(3), 143–153.

Van Driel, C., Hoedemaeker, M., & Van Arem, B. (2007). Impacts of a congestion assistant on driving behaviour and acceptance using a driving simulator. *Journal of Transportation Research F*, *10*, 139–152.

Venhovens, P., Naab, K., & Adiprasito, B. (2000). Stop and Go cruise control. *International Journal of Automotive Technology*, *1*(2), 61–69.

Widmann, G., Daniels, M., Hamilton, L., Humm, L., Riley, B., Schiffmann, J., et al. (2000). Comparison of lidar-based and radar-based adaptive cruise control systems. *SAE technical paper series* (2000-01-0345).

Yanakiev, D., Eyre, J., & Kanellakopoulos, I. (1998). *Analysis, design and evaluation of AVCS for heavy-duty vehicles with actuator delays*. California PATH Research Report (UCB-ITS-PRR-98-18).

Zhang, J., & Ioannou, P. (2004). *Integrated roadway/adaptive cruise control system: Safety performance environmental and near term deployment considerations*. California PATH Research Report (UCB-ITS-PRR-2004-32).